

Geometry of the Turkey-Arabia and Africa-Arabia plate boundaries in the latest Miocene to Mid-Pliocene: the role of the Malatya-Ovacık Fault Zone in eastern Turkey

R. Westaway^{1,*}, T. Demir², and A. Seyrek³

¹Faculty of Mathematics and Computing, The Open University, Eldon House, Gosforth, Newcastle-upon-Tyne NE3 3PW, UK

²Department of Geography, Harran University, 63300 Şanlıurfa, Turkey

³Department of Soil Science, Harran University, 63300 Şanlıurfa, Turkey

* also at: IRES, Newcastle University, Newcastle-upon-Tyne NE1 7RU, UK

Received: 27 August 2007 – Published in eEarth Discuss.: 22 November 2007

Revised: 18 March 2008 – Accepted: 15 July 2008 – Published: 5 August 2008

Abstract. We suggest a working hypothesis for the geometry of the strike-slip faults that formed the boundaries between the Turkish, African and Arabian plates in the latest Miocene to Mid-Pliocene (LMMP), between ~ 7 – 6 Ma and ~ 3.5 Ma. This geometry differed significantly from the modern geometry; the northern Dead Sea Fault Zone (DSFZ) was located east of its present line and the TR-AR boundary was formed by the Malatya-Ovacık Fault Zone (MOFZ), located well north of the modern East Anatolian Fault Zone (EAFZ). The MOFZ is potentially the most problematic aspect of such a scheme, given the dramatically different interpretations of it that have been proposed. However, the presently-available evidence, albeit limited, is consistent with our proposed interpretation. Significant differences between the proposed LMMP fault geometry and the modern geometry include, first, the transtensional geometry of the MOFZ, the modern EAFZ being typically a left-lateral transform fault zone but with localized transpression. Second, the MOFZ slip rate was much lower than the ~ 9 – 10 mm a⁻¹ EAFZ slip rate; it is estimated as ~ 2 – 3 mm a⁻¹, having produced no more than ~ 8 km of slip during its approximately three million year long activity. The Euler vector is tentatively inferred to have involved relative rotation between the Turkish and Arabian Plates at $\sim 0.85 \pm 0.15^\circ$ Ma⁻¹ about a pole at $\sim 37.75 \pm 0.15^\circ$ N, $\sim 38.8 \pm 0.3^\circ$ E. Third, unlike at present, there was no throughgoing linkage of left-lateral faulting between the LMMP DSFZ and the MOFZ; instead, the DSFZ terminated northward, and the

MOFZ terminated southward, in a zone of localised crustal shortening adjoining the suture of the former Neotethys Ocean in the Kahramanmaraş-Pazarcık region of SE Turkey. The different motion of the Turkish plate relative to Arabia, and, thus, relative to Eurasia, means that senses and rates of crustal deformation can be expected to have been different during the LMMP phase from at present, throughout the eastern Mediterranean region.

1 Introduction

Eastern Turkey forms the modern boundary zone between the African (AF), Arabian (AR), Eurasian (EU) and Turkish (TR) plates (Fig. 1). The right-lateral North Anatolian Fault Zone (NAFZ) takes up westward motion of the Turkish plate relative to Eurasia; the left-lateral East Anatolian Fault Zone (EAFZ) accommodates WSW motion of the Turkish plate relative to Arabia. The overall effect of both fault systems is to accommodate NNW motion of Arabia relative to Eurasia by westward motion of the Turkish plate. This modern geometry of the NAFZ and EAFZ, which converge at Karlıova (Fig. 1), is thought to have developed in the Mid-Pliocene (e.g., Westaway, 2003, 2004, 2006; Westaway et al., 2006).

Most of the NAFZ is thought to have come into being in the late Late Miocene, around 7 Ma or thereabouts (e.g., Tüysüz et al., 1998; Armijo et al., 1999; Yalıtırak et al., 2000; Westaway, 2003, 2004, 2006; Westaway et al., 2005). However, during the latest Miocene – Mid-Pliocene (LMMP) the regional kinematics were different from at present; it has been proposed (e.g., Westaway and Arger, 2001) that the



Correspondence to: R. Westaway
(robwestaway@tiscali.co.uk)

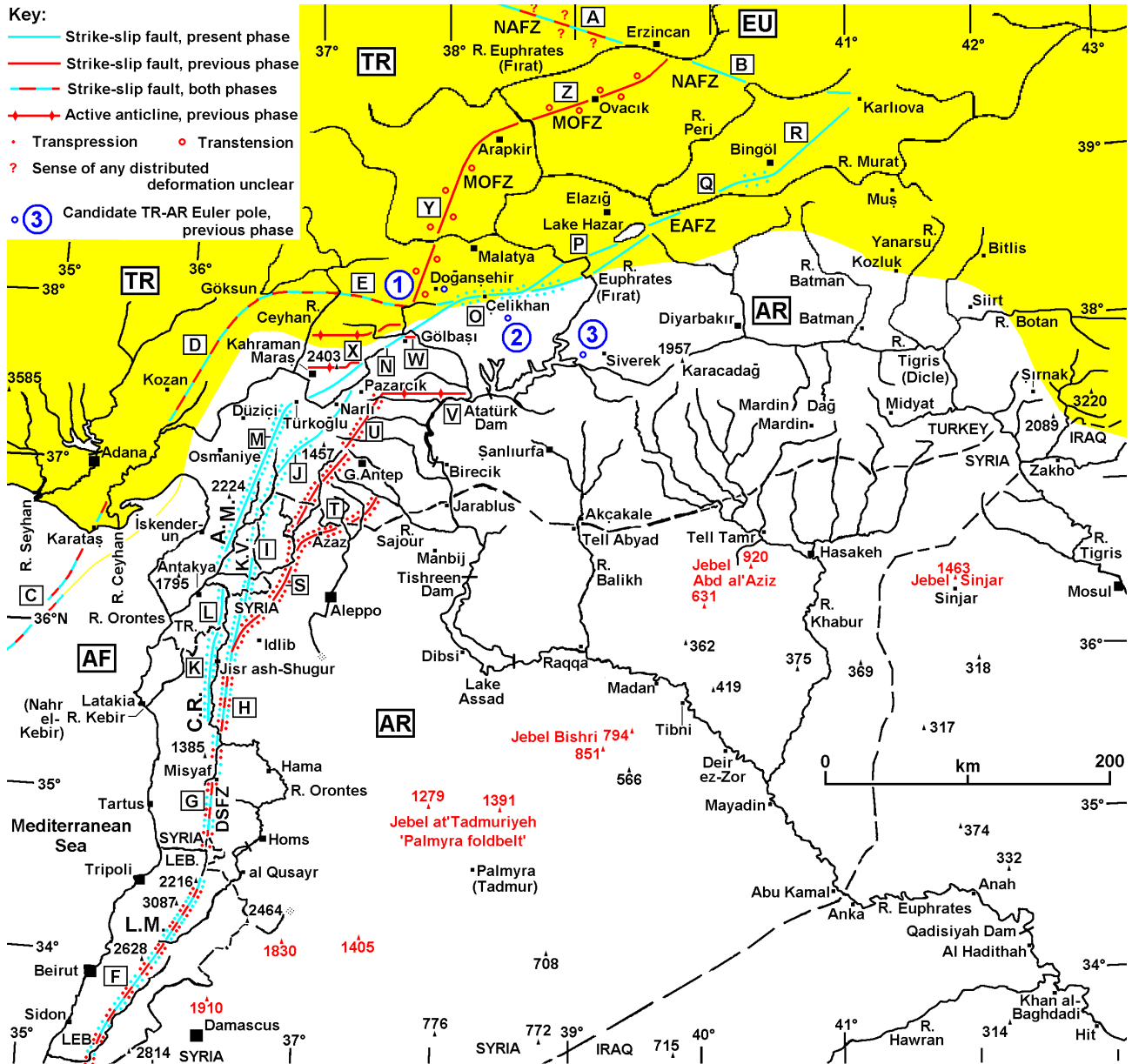


Fig. 1. Regional map showing the location of the study area in relation to the rivers Tigris and Euphrates and the active strike-slip faults (simplified from Westaway, 2004, which lists original sources of information) bounding the Arabian (AR), African (AF), Turkish (TR), and Eurasian (EU) plates. DSFZ, EAFZ and NAFZ denote the Dead Sea Fault Zone (left-lateral), East Anatolian Fault Zone (left-lateral), and North Anatolian Fault Zone (right-lateral), respectively. Lake Hazar occupies a pull-apart basin on the EAFZ. Note right-lateral offsets of the rivers Euphrates and Peri across the NAFZ and left-lateral offsets of the rivers Euphrates and Murat across the EAFZ. Mountain ranges forming as a result of distributed shortening along the DSFZ are labelled thus: L. M., the Lebanon Mountains; C. R., the Syrian Coastal Range (Jebel Nusayriyah); A. M., the Amanos Mountains. K. V. denotes the Karasu Valley. G. Antep is an abbreviation for Gaziantep. The suture of the Neotethys Ocean follows the change from yellow to colourless ornament at the boundary between Anatolia and the Arabian Platform. The meaning and significance of letters to denote individual faults and other structures are discussed in the text.

eastern end of the NAFZ was at Erzincan, not at Karliova, and this structure was conjugate to a different left-lateral fault system, the Malatya-Ovacık Fault Zone (MOFZ) (Figs. 1, 2), although this idea has since been criticised (Kaymakçı et al., 2006). The aims of this study are to suggest a

working hypothesis for the geometry of plate motion during the LMMP and to investigate the extent to which the MOFZ (which, admittedly, is potentially the most problematic aspect of the scheme) is consistent with the proposal.

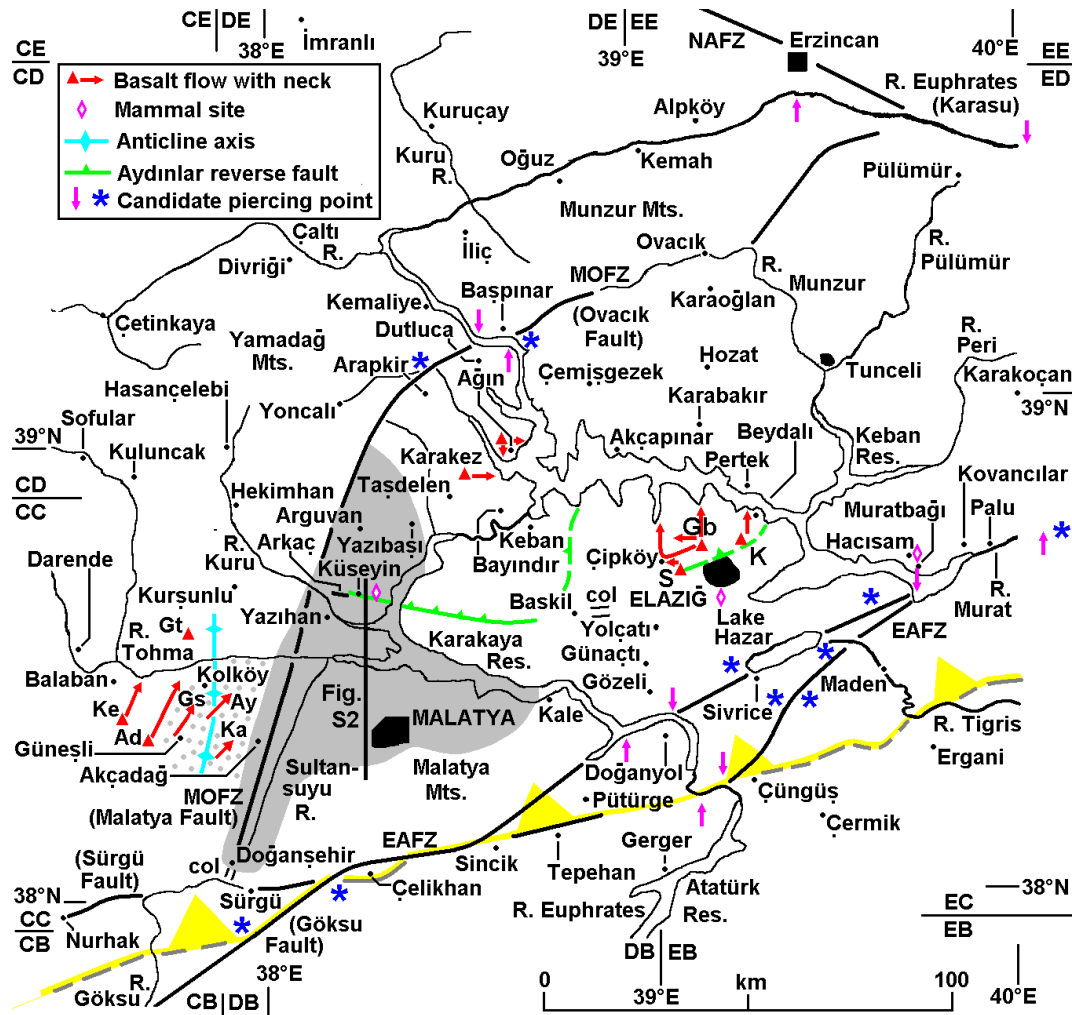


Fig. 2. Map of the study region, showing sites of (?) Late Miocene – Pliocene basaltic volcanism (triangles; omitted outside the Elazığ region) in relation to the Euphrates river system and to major strike-slip fault zones: the NAFZ, MOFZ and EAFZ. Light grey shading illustrates schematically the Malatya Basin. Large light grey dots indicate the estimated extent of such deposits in the swath of territory west of the Malatya Fault that we have investigated (see supplement for details: <http://www.electronic-earth.net/3/27/2008/ee-3-27-2008-supplement.pdf>). Mammal sites illustrated include Karababa in the Malatya Basin (see supplement for details) and (from Ünay and de Bruijn, 1998) Sürsürü near Elazığ and Hacısam farther east. Dashed dark grey line with yellow ornament marks the Neotethys suture, as delimited by the northern margin of outcrop of rocks of the Cenozoic carbonate sequence of the Arabian Platform (after Altınlı, 1961; Baykal, 1961; and Tolun, 1962). Between points marked, this suture roughly coincides with strands of the EAFZ. Triangles indicate young basaltic necks, with arrows indicating schematic directions of basalt flow from them; Gb, K and S denote the Gümüşbağlar, Karataş, and Sarıbuçuk necks near Elazığ. Ke, Ad, Gs, Ay, Ka and Gt indicate the Kepezdağı, Adamkıran, Güneşli, Aygörmez Dağı, Karaca Dağ and Göktepe flow units of the Kepezdağı basalt. For geological maps of this area see Westaway and Arger (2001). Thick black line indicates the location of the cross-section in Fig. S2 in the online supplement. Arrow symbols denote piercing points from river offsets; * symbols denote possible piercing points from structural evidence. Those on the NAFZ and EAFZ are not discussed here; see, instead, Westaway and Arger (2001) and Westaway (2003, 2004).

2 Geometry of the Turkey-Arabia and Africa-Arabia plate boundaries

2.1 Present geometry of deformation

The fault zones coloured blue in Fig. 1 indicate the modern plate-boundary geometry. The summary here follows recent interpretations, such as by Westaway (2003, 2004) and

Westaway et al. (2006), which discuss alternative possible scenarios, discussion that is not repeated here. Westaway and Arger (2001) summarised the earlier literature on the age of this fault system, and concluded that it was ~3 Ma. Westaway (2003) revised this estimate to ~4 Ma; subsequent more detailed analysis by Westaway et al. (2006) adjusted it to 3.73 ± 0.05 Ma.

The NAFZ enters the study region with an ESE trend (A in Fig. 1). It continues ESE past Erzincan, offsetting the Euphrates and Peri rivers right-laterally (B), before ending at its intersection with the EAFZ at Karlıova.

The modern left-lateral boundary between the Turkish and African plates trends NE across the NE Mediterranean Sea, where it is known as the Misis-Kyrenia fault zone (C). It then passes onshore, end-on, into the similarly-oriented Yakapınar-Göksun fault zone (D). Near its NNE end the latter bends to a west-east orientation and, now known as the Sürgü Fault (E), continues eastward to the vicinity of Doğanşehir, beyond which it merges into the EAFZ.

The modern configuration of the northern Dead Sea Fault Zone (DSFZ) comprises, as its principal active strand, the NNE-trending Yammouneh Fault (F), which bounds the eastern margin of the Lebanon mountain range and the western margin of the Bekaa Valley. On leaving Lebanon and entering Syria the active left-lateral displacement passes end on into the north-trending Misyaf Fault (G), which continues end on into the Apamea Fault (H). As Seyrek et al. (2007) have shown, roughly half the active displacement then passes end-on, northward, onto the Armanaz Fault and then the East Hatay Fault (I), which follows the eastern margin of the Karasu Valley, continuing NNE on other active faults to the vicinity of Narlı in SE Turkey (J). The rest steps leftward from the Apamea Fault, across the Ghab Basin, onto another fault that bounds the eastern margin of the Jebel Nusayriyah mountain range (K), which passes northward, end-on, in the vicinity of Jisr esh-Shugur into the Qanaya-Babatorun Fault (L). This component of displacement then again steps leftward, across the Amik Basin, onto the Amanos Fault (M), which continues NNE to the vicinity of Türkoğlu, bounding the western margin of the Karasu Valley and the eastern margin of the Amanos mountain range. This component of displacement then passes end-on onto the NE-trending Gölbaşı-Türkoğlu Fault (N), which merges with the Sürgü Fault (E) at its NE end.

The northern end of the DSFZ thus passes end-on into the SW end of the EAFZ in the Kahramanmaraş region of SE Turkey, as discussed by Westaway (2003, 2004). However, a minor component of the EAFZ slip splays westward, north of this area, and passes via the aforementioned Sürgü Fault (E) onto the TR-AF plate boundary. The EAFZ has a general WSW-ENE trend, but locally trends W-E in the vicinity of Çelikhhan (O) as it threads its way across the suture of the former Neotethys Ocean that forms the boundary between the Arabian Platform and Anatolia. It then continues ENE as the en echelon Hazar-Şiro fault (which steps leftward across the Lake Hazar pull-apart basin) and Çüngüş fault (P), both of which offset the River Euphrates, before merging as the Palu Fault (Q) that offsets the River Murat, and which passes end-on onto the Göynük Fault (R) that meets the NAFZ at the Karlıova triple junction.

2.2 Relationship to the earlier phase of deformation

As already noted, the NAFZ is thought to have become active during the Messinian stage of the Late Miocene, although opinions have differed (cf. Tüysüz et al., 1998; Armijo et al., 1999; Yaltrak et al., 2000; Westaway, 2003) as to whether its initiation was around the start of the Messinian, at ~ 7 Ma, or in the “latest Miocene” (i.e., during the Messinian, therefore probably closer to a numerical age of ~ 6 Ma). The NAFZ is thus older than the modern configuration of the northern DSFZ and the EAFZ. This raises the obvious question regarding the location of the LMMP TR-AR and AF-AR plate boundaries. Westaway and Arger (1996) first suggested that at this time the TR-AR boundary was the MOFZ, consisting of the Malatya Fault (Y in Fig. 1) and the Ovacık Fault (Z in Fig. 1); Westaway and Arger (2001) subsequently developed this idea into a quantitative kinematic model, which included estimation of a MOFZ Euler pole some 1400 km to the southeast (i.e., in the vicinity of Lat. 30° N, Long. 50° E, near the head of the Persian Gulf).

Both the Malatya and Ovacık faults were first recognized long ago (e.g., by Arpat and Şaroğlu, 1975). The principal evidence for the Malatya Fault was a major linear escarpment along the WNW margin of the Malatya Basin (Fig. 2), a Late Cenozoic lacustrine basin (e.g., Önal, 1995, 1997) in eastern Anatolia. Evidence for the Ovacık Fault is provided, first, by the ENE-trending lineation of the Ovacık valley at the SSE margin of the ~ 3400 m high Munzur mountain range. Second, beyond the WSW end of the Ovacık valley, several rivers, including the Euphrates (Fig. 2), are offset left-laterally by concordant distances of ~ 8 km.

Moreover, previous studies (e.g., Özgül, 1976; Perinçek and Kozlu, 1984) have recognised the crustal blocks on either side of the MOFZ as distinct terranes, which accreted together to form eastern Anatolia. The different crustal properties are reflected in the present-day crustal thickness: ~ 42 km around Elazığ, SE of the MOFZ; but ~ 50 km NW of the MOFZ (Zor et al., 2003), and in an abrupt variation in related geophysical observables such as the surface heat flow (e.g., Tezcan, 1995) and the Bouguer gravity anomaly (e.g., Ateş et al., 1999). One can thus readily envisage that, when strike-slip faulting first developed in this region in the latest Miocene, it exploited such an ancient inherited line of weakness, rather than cutting through previously intact rock.

Nonetheless, it is now clear (in part from the new data presented by Kaymakçı et al., 2006, and in part from our own original fieldwork) that some of the supporting evidence used by Westaway and Arger (2001) to infer the kinematics of the MOFZ is invalid; however, it is also clear that Kaymakçı et al. (2006) were unable to relate the evidence that they reported to the wider regional context. We thus accept that the MOFZ is at present the most problematic aspect of the wider regional kinematics, but to avoid discussion of local detail about it

overwhelming the regional picture, this discussion is placed in our online supplement (<http://www.electronic-earth.net/3/27/2008/ee-3-27-2008-supplement.pdf>).

The evidence now available pertaining to the role of the MOFZ can be summarized as follows. First, it consists of the SSW-striking Malatya Fault (Y in Fig. 1) and the ENE-trending Ovacık Fault (Z in Fig. 1), as previously suggested. Second, for most of their lengths these faults have accommodated left-lateral transtension. Third, the key constraint on their total slip arises from the ~8 km left-lateral offset of the gorge of the River Euphrates between Dutluca and Başpınar (Fig. 2). Fourth, dating of sediments in the Malatya Basin, overlying and adjoining the Malatya Fault, can in principle constrain the timing of slip on this structure. However, this sedimentary succession represents a much greater span of time than the activity on this fault. It is indeed evident that deposition early in the succession persisted for tens of kilometres west of the Malatya Fault; the shape of the basin was subsequently modified by anticlinal folding (illustrated schematically in pale blue in Fig. 2), which we infer was synkinematic with the transtension on the Malatya Fault. Conversely, components of reverse-faulting and related localised folding in the area east of the MOFZ and north of the EAFZ (shown in green in Fig. 2) are inferred by us to relate to the present phase of deformation (i.e., they involve minor components of internal deformation of the modern Turkish plate) and are thus unrelated to the slip on the MOFZ (cf. Kaymakçı et al., 2006). Finally, there is no evidence to contradict the suggestion that the MOFZ was active between the latest Miocene and Mid-Pliocene, as tentatively proposed by Westaway and Arger (2001).

Regarding the AF-AR boundary, it is now evident that its northernmost segment, formed by the Amanos and East Hatay faults (I and M in Fig. 1) did not become active until the Mid-Pliocene (e.g., Seyrek et al., 2007, 2008), superseding previous views that it is of much greater antiquity. However, it is clear that the modern AF-AR plate boundary in western Syria is older; as Westaway (2003) pointed out, basalt flows associated with the ~6–5 Ma Homs basalt cascade into the linear valley along this fault zone, which thus already existed at the time. Structural and geomorphic lineations indicative of an array of now inactive left-lateral faults are known in the Turkey-Syria border region around the city of Gaziantep (T in Fig. 1). It can thus be inferred that the LMMP AF-AR plate boundary passed northward from NW Syria onto this array of faults, illustrated in red in Fig. 1.

We thus infer that, between the latest Miocene and Mid-Pliocene, slip on the Apamea Fault (H) within the DSFZ passed, end-on, NNE onto the Afrin Fault (S), located to the east of the modern AF-AR plate boundary zone. Displacement passed from there, end-on, onto the array of en echelon faults in the vicinity of Gaziantep (T), only the most westerly and easterly members of which are shown in Fig. 1 (see Westaway, 2004, for more detail). Displacement passed

from there onto the Kırkpınar Fault (U), which continues NNE to the vicinity of Pazarcık, some 50 km south of the southern end of the MOFZ (Fig. 1). Faults in this set appear to terminate against anticlines located on their eastern side; for instance, the Kırkpınar Fault seems to terminate against the Suvarlı anticline (V in Fig. 1). This area has been affected by dramatic Late Cenozoic folding, shown schematically in Fig. 1, which pre-dates the modern geometry of the EAFZ (e.g., Westaway and Arger, 1996; Westaway et al., 2006) and can thus be inferred to be synkinematic, at least in part, with the LMMP AF-AR plate boundary.

Since there is no contrary evidence, we infer, in addition, that the LMMP boundary between the Turkish and African plates was in the same place as at present (i.e., C-D-E in Fig. 1). Such an interpretation is consistent with the deduction by Robertson et al. (2004) that left-lateral slip on the Yakapınar-Göksun Fault Zone (D in Fig. 1) became active in the Messinian, thus constraining the start of the LMMP phase of deformation independently of evidence from the NAFZ. This implies that the contemporaneous left-lateral slip on the Sürgü Fault (D) accompanied crustal shortening across the anticlines to the north of Kahramanmaraş (including the Ahır and more northerly Engizek anticlines, X in Fig. 1), thus partitioning the contemporaneous relative motion between the Turkish and Arabian plates. Subsequently, during the present phase of deformation, the Ahır anticline (X) has been truncated by the Gölbaşı-Türkoğlu Fault (N); its eastern part is evident to the east of the latter fault, north of Gölbaşı (W), as discussed by Westaway and Arger (1996) and Westaway et al. (2006). If this young left-lateral slip is restored to juxtapose the two anticline fragments, the overall geometry envisaged for the LMMP phase of deformation can be more easily visualised.

East of the marked strands of the northern DSFZ, a succession of fold mountains (labelled in red in Fig. 1) extends across central and NE Syria and NW Iraq. These folded structures are thought to be underlain by blind reverse faults that have accommodated a significant component of the northward motion of Arabia. There is a substantial literature on this topic (e.g., McBride et al., 1990; Chaimov et al., 1992; Alsdorf et al., 1995; Litak et al., 1997) but it provides insufficient chronological resolution for the purposes of the present study (i.e., it cannot resolve deformation during the LMMP from deformation during the present phase of plate motions or deformation while the southern DSFZ was active, before the LMMP phase). However, one such structure (the Jebel Bishri) is transected by the River Euphrates; Demir et al. (2007) have shown that the older (?) Mid-Pliocene terraces of this river are significantly warped across this structure, suggesting that such structures accommodated significant crustal shortening during the LMMP.

Finally, if one restores the ~35 km of SW translocation of the Turkish plate relative to the Arabian plate, which has occurred while the EAFZ has been active (e.g., Westaway,

Table 1. MOFZ kinematic models.

Site	UTM	α_F	D (km)	α ($^\circ$)	θ ($^\circ$)	$\Delta\alpha$ ($^\circ$)	V (mm/a)	U (km)	U_L (km)	U_E (km)
Euler vector 2.2°Ma^{-1} about [DC 035 160] (i.e., $38^\circ 05' \text{N}$, $37^\circ 54' \text{E}$; pole 1)										
Kahramanmaraş	CB 170 625	N 80°E	101.7	238.3	148.3	21.7	3.91	11.72	-4.34	-10.88
Doğanşehir	DC 015 170	N 20°E	2.2	296.6	206.6	83.4	0.09	0.26	0.26	0.03
Akcadağ	DC 130 445	N 20°E	30.0	18.4	288.4	1.6	1.15	3.46	0.09	3.46
Yazihan	DC 240 760	N 20°E	63.4	18.9	288.9	1.1	2.43	7.30	0.14	7.30
Arguvan	DC 370 930	N 30°E	84.0	23.5	293.5	6.5	3.22	9.67	1.09	9.61
Arapkir	DD 555 255	N 50°E	121.2	25.4	295.4	24.6	4.65	13.96	5.81	12.70
Başpınar	DD 720 360	N 60°E	138.2	29.7	299.7	30.3	5.31	15.92	8.03	13.74
Ovacık	ED 110 560	N 70°E	176.5	37.5	307.5	32.5	6.78	20.33	10.92	17.15
Euler vector 1.1°Ma^{-1} about [DB 560 900] (i.e., $37^\circ 51' \text{N}$, $38^\circ 30' \text{E}$; pole 2)										
Kahramanmaraş	CB 170 625	N 80°E	141.7	258.8	168.8	1.2	2.72	8.16	-0.17	-8.16
Doğanşehir	DC 015 170	N 20°E	60.8	296.4	206.4	83.6	1.17	3.50	3.48	0.39
Akcadağ	DC 130 445	N 20°E	69.4	321.7	231.7	58.3	1.33	4.00	3.40	2.10
Yazihan	DC 240 760	N 20°E	91.8	339.6	249.6	40.4	1.76	5.29	3.43	4.02
Arguvan	DC 370 930	N 30°E	104.7	349.5	259.5	40.5	2.01	6.03	3.91	4.59
Arapkir	DD 555 255	N 50°E	135.5	359.8	269.8	50.2	2.60	7.80	6.00	4.99
Başpınar	DD 720 360	N 60°E	146.9	6.3	276.3	53.7	2.82	8.46	6.82	5.00
Ovacık	ED 110 560	N 70°E	174.9	18.3	288.3	51.7	3.36	10.07	7.90	6.25
Euler vector 0.8°Ma^{-1} about [EB 090 620] (i.e., $37^\circ 36' \text{N}$, $39^\circ 06' \text{E}$; pole 3)										
Kahramanmaraş	CB 170 625	N 80°E	192.0	270.1	0.1	169.9	2.68	8.04	1.42	-7.92
Doğanşehir	DC 015 170	N 20°E	120.8	297.1	207.1	82.9	1.69	5.06	5.02	0.62
Akcadağ	DC 130 445	N 20°E	126.6	310.7	220.7	69.3	1.77	5.30	4.96	1.87
Yazihan	DC 240 760	N 20°E	142.2	323.3	233.3	56.7	1.99	5.96	4.98	3.27
Arguvan	DC 370 930	N 30°E	149.5	331.2	241.2	58.8	2.09	6.26	5.36	3.24
Arapkir	DD 555 255	N 50°E	172.0	341.9	251.9	68.1	2.40	7.21	6.69	2.69
Başpınar	DD 720 360	N 60°E	177.9	348.0	258.0	72.0	2.48	7.45	7.09	2.30
Ovacık	ED 110 560	N 70°E	194.0	0.6	270.6	69.4	2.71	8.13	7.61	2.86

2004), one finds the zone of crustal shortening in the Kahramanmaraş-Pazarçık area to be located at a rightward step between the northern end of the LMMP AF-AR plate boundary and the southern end of the MOFZ (Fig. 1). Such a component of localized crustal shortening is to be expected at a rightward step in left-lateral faulting. Moreover, such a geometry would also enable the component of left-lateral slip on the MOFZ to transfer southward onto the AF-AR plate boundary, in the process crossing the Neotethys suture at the boundary between the Arabian Platform and the Anatolian crustal province (Fig. 1). This geometry thus solves what Westaway and Arger (2001) saw as a major outstanding problem with the MOFZ kinematics: the fact that it clearly has no throughgoing southward left-lateral continuation. The geometry of faulting envisaged in Fig. 1 thus provides, for the first time, a testable working hypothesis for the overall LMMP plate-boundary geometry in this region.

3 Revised kinematic model for the MOFZ

We now investigate possible quantitative solutions for the MOFZ kinematics, by considering Euler vectors that may

account for the available evidence. We shall try to account for the components of left-lateral transtension across both the Malatya and Ovacık faults, despite their different orientations, and for the left-lateral slip of ~ 8 km at the point where the Euphrates gorge has been offset (Fig. 2). We show that these forms of evidence can be accommodated if the Euler pole to the MOFZ is adjusted much closer to the MOFZ than Westaway and Arger (2001) envisaged, with a corresponding adjustment in the rate of anticlockwise rotation of the Turkish plate relative to Arabia.

For the first solution, the Euler pole to the MOFZ is placed near its southern end (i.e., near Doğanşehir; Fig. 2; pole 1 in Fig. 1 and Table 1). This results in the prediction of extension and minor left-lateral slip on the southern Malatya Fault at rates that increase northward. Farther north, it predicts a combination of left-lateral slip and extension, the proportion of left-lateral slip increasing as the fault zone bends to the ENE. Predicted rates of relative motion also increase northward and eastward, away from this pole. Such a solution could thus explain why the Malatya Fault has no southward continuation past Doğanşehir (cf. Westaway and Arger, 2001): this locality adjoins the MOFZ Euler pole

so local TR-AR relative motion was minimal and thus no major structure was needed to accommodate it. This solution also predicts TR-AR relative motion towards the SSE in the Kahramanmaraş area farther SW (Fig. 1), where dramatic folding across ENE-trending anticlines preceded the local development of the EAFZ (cf. Westaway and Arger, 1996; Westaway et al., 2006b). However, elsewhere the solution is not so satisfactory; for instance to match the Euphrates river offset it requires many kilometres of local extension, for which there is no evidence (cf. Westaway and Arger, 2001).

Table 1 thus considers a second possible solution, with the TR-AR Euler pole now near Adıyaman (pole 2 in Fig. 1), ~ 60 km ESE of the previous alternative. This predicts TR-AR motion more closely perpendicular to the anticline axes in the Kahramanmaraş area and also achieves a reasonable match to the observed left-lateral offset of the Euphrates, predicting less extension both in the southern Malatya Basin and around Ovacık. Thus, although the extension across the Malatya Fault decreases to zero at its southern end, its left-lateral slip decreases no lower than ~ 3 km, implying that the southernmost Malatya Fault took up almost pure left-lateral slip. This solution thus achieves a better overall fit to the observational evidence.

Table 1 also shows a third solution, for an Euler pole another ~ 60 km farther ESE, near Hilvan (pole 3 in Fig. 1). Compared with solution 2, this would imply greater proportions of left-lateral slip to extension on most of the MOFZ, but is not fundamentally different.

While accepting that no model of this type can account for every local detail, it seems clear that solutions 2 and 3 (Table 1) represent viable kinematic models for the MOFZ. At this stage the MOFZ Euler vector cannot be determined with precision, but it now seems evident that its pole lay quite close to the southern end of the MOFZ, probably not far south or southeast of Malatya. Taking account of the differences between solutions 2 and 3 in Table 1, we tentatively estimate that the Euler vector involved relative rotation at $\sim 0.85 \pm 0.15^\circ \text{Ma}^{-1}$ about a pole at $\sim 37.75 \pm 0.15^\circ \text{N}$, $\sim 38.8 \pm 0.3^\circ \text{E}$.

4 Discussion

The above analysis suggests that the Malatya and Ovacık faults were both transtensional, but with left-lateral slip predominant over extension. In solution 3, the lowest ratio of extension to left-lateral slip is evident in the vicinity of the offset reach of the River Euphrates. However, the evidence (see the online supplement: <http://www.electronic-earth.net/3/27/2008/ee-3-27-2008-supplement.pdf>, also Westaway and Arger, 2001) suggests that the N 60° E–S 60° W offset of the Euphrates gorge may have been purely left-lateral. One could thus argue instead for an alternative solution strategy, to constrain the MOFZ pole to lie S 30° E from this offset, to force such a constraint. Pole 3 in Table 1 in fact lies at an

azimuth of S 27° E from this locality, so a small adjustment (say, ~ 5 km NNE, to [EB 093 624]) would predict that the Euphrates river offset was purely left-lateral but keep the predictions of extension and strike-slip elsewhere on the MOFZ very similar to those already derived for the existing solution 3.

In the Kahramanmaraş area, west of MOFZ pole 3 (Fig. 1), solution 3 predicts that the southward motion of the Turkish plate relative to Arabia was partitioned with ~ 7 km of N-S crustal shortening and ~ 1.5 km of E-W left-lateral slip. As already noted, we infer that such a component of shortening was accommodated on E-W-trending anticlines, such as those now forming the Ahır and Engizek mountain ranges (X in Fig. 1), and that the component of left-lateral slip was taken up on the Sürgü Fault (Fig. 1). It follows that the Sürgü Fault was indeed already active at this time, implying that the geometry of the LMMP TR-AF plate boundary was the same as at present. Furthermore, if the total slip of ~ 4 km on the Sürgü Fault is partitioned with ~ 1.5 km during the LMMP phase and ~ 2.5 km since, the total predicted TR-AR relative motion since the EAFZ became active is ~ 1.5 km less than was previously thought. It follows (by working again through the detailed reasoning set out by Westaway et al. (2006), but with the above smaller value of TR-AF motion) that the best estimate of the EAFZ age adjusts slightly downward, to ~ 3.6 Ma, a formal estimate (using the same analysis procedure as Westaway et al. (2006), but with 35.5 km of total slip at the SW end of the EAFZ instead of 37 km) being 3.58 ± 0.05 Ma.

The realization that the Malatya Basin was transtensional while the MOFZ was active also has wider significance. It is now generally accepted that the Sea of Marmara, on the NAFZ near İstanbul, is an active transtensional basin (e.g., Armijo et al., 2002). Investigation of the detailed nature of the deformation occurring in and around the Sea of Marmara is important to determine the local stress field, and thus to investigate the earthquake hazard to this city. However, the detailed geometry of the structures now active beneath the Sea of Marmara is difficult to study, due to being underwater, and has been disputed (cf. Le Pichon et al., 2001). The Malatya Basin is potentially a more accessible analogue that may reveal detail inaccessible in the Sea of Marmara.

It is evident that the Cenozoic continental collision between Anatolia and the Arabian Platform has resulted in much greater deformation of the former than of the latter. As Demir et al. (2007) have noted, abundant evidence (e.g., from igneous petrology and seismic profiling) indicates that the Arabian Platform crust has a thick basal layer of mafic material that has been emplaced by magmatic underplating. Such a layer will limit the temperature within the overlying crust, restricting the rate at which it can deform, and seems to be the principal cause of the dramatic difference in strength between these crustal provinces. Figure 1 indicates that the entire SE boundary of the LMMP Turkish plate was located within the weaker crust of Anatolia, where it was presumably

relatively easy for faulting to develop. At this time (in contrast with at present) there was evidently no throughgoing linkage between the strike-slip faults forming this boundary of the Turkish plate and those forming the AF-AR plate boundary. However, as already noted, both these boundaries were in close proximity; N-S crustal shortening indeed seems to have been necessary in the Kahramanmaraş area, both to provide a northward termination of the DSFZ against the northern margin of the Arabian Platform and to facilitate the TR-AR relative motion by slip on the MOFZ. Conversely, the modern geometry of faulting (Fig. 1) involves throughgoing linkage between the DSFZ and the EAFZ. Unlike the MOFZ, the southern part of the EAFZ is within the relatively strong crust of the Arabian Platform, south of the Neotethys suture. To reach this locality the EAFZ crosses the suture near Çelikhhan by stepping to the right and reactivating part of the suture as a left-lateral fault within a localized zone of transpression (Fig. 1). Such reactivation of an ancient line of weakness is similar in principle to the reactivation that, we suggest, led to the development of the MOFZ during the LMMP phase.

Many fundamental questions about the strike-slip faulting in the present study region evidently remain to be answered. For instance, is the proposed MOFZ Euler vector compatible with the LMMP kinematics of the NAFZ, for instance, regarding the differences relative to the present-day kinematics envisaged by Westaway (2006) in localities adjoining the western NAFZ? Can it be demonstrated that the LMMP strike-slip faulting became active during the Messinian salinity crisis, thus favouring the causal mechanism tentatively suggested by Westaway (2003)? What was the slip rate on the LMMP northern DSFZ, given that a significant part of the northward motion of Arabia seems at this time to have been accommodated on other structures farther east (see Fig. 1 and its caption)? Is there indeed any simple connection between the low slip rate estimated on the MOFZ (Table 1) and the fact that only part of the contemporaneous northward motion of Arabia was accommodated on the northern DSFZ (the rest having been evidently accommodated by distributed deformation across eastern Syria)? What caused the switch from the LMMP plate-boundary geometry to the present geometry? Might it relate to difficulties in the LMMP geometry accommodating large amounts of relative motion, for instance at the NAFZ-MOFZ intersection, as suggested by Westaway and Arger (2001), or at the western end of the NAFZ, as suggested by Westaway (2006)? Is it possible that the critical locality was instead in the vicinity of Kahramanmaraş where, as is now evident (Fig. 1), the LMMP geometry required such intense localized deformation? The EAFZ in the Çelikhhan-Gölbaşı-Türkoğlu area (Fig. 1) is indeed oriented close to the direction of maximum resolved left-lateral shear stress that the LMMP crustal shortening would have created. Such issues are beyond the scope of this study, but will be addressed by other work in future.

5 Conclusions

We have suggested a working hypothesis, illustrated in Fig. 1, for the geometry of the strike-slip faults that bounded the Turkish, African and Arabian plates in the latest Miocene to Mid-Pliocene, active between ~ 7 -6 Ma and ~ 3.5 Ma. This geometry differed significantly from the modern geometry; the northern DSFZ was located east of its present line and the TR-AR boundary was formed by the MOFZ, located well north of the modern EAFZ. The MOFZ is potentially the most problematic aspect of such a scheme, given the dramatically different interpretations of it that have been proposed. However, we have shown that the available evidence, albeit limited, is consistent with our proposed interpretation. Significant differences between the proposed LMMP fault geometry and the modern geometry include, first, the transtensional geometry of the MOFZ, the modern EAFZ being typically a left-lateral transform fault zone with localized transpression. Second, the MOFZ slip rate was much lower than the ~ 9 -10 mm a⁻¹ EAFZ slip rate; it is estimated as ~ 2 -3 mm a⁻¹, having produced no more than ~ 8 km of slip during its approximately three million year long activity. The Euler vector is tentatively inferred to have involved relative rotation between the Turkish and Arabian Plates at $\sim 0.85 \pm 0.15^\circ$ Ma⁻¹ about a pole at $\sim 37.75 \pm 0.15^\circ$ N, $\sim 38.8 \pm 0.3^\circ$ E. Third, unlike at present, there was no throughgoing linkage by left-lateral faulting between the LMMP DSFZ and the MOFZ; instead, the DSFZ terminated northward, and the MOFZ terminated southward, in a zone of localised crustal shortening adjoining the suture of the former Neotethys Ocean in the Kahramanmaraş-Pazarcık region of SE Turkey. The different motion of the Turkish plate relative to Arabia, and, thus, relative to Eurasia, means that senses and rates of crustal deformation can be expected to have been different during this LMMP phase from at present, throughout the eastern Mediterranean region.

Edited by: J. Smit

References

- Alsdorf, D., Barazangi, M., Litak, R., Seber, D. Sawaf, T., al-Saad, D.: The intraplate Euphrates Depression - Palmyrides Mountain Belt junction and relationship to Arabian plate boundary tectonics, *Annali di Geofisica*, 38, 385-397, 1995.
- Altunli, İ. E.: Erzurum sheet of the Geological Map of Turkey, 1:500,000 scale, General Directorate of Mineral Research and Exploration, Ankara, 1961.
- Armijo, R., Meyer, B., Hubert, A., and Barka, A.: Westward propagation of the North Anatolian fault into the northern Aegean: Timing and kinematics, *Geology*, 27, 267-270, 1999.
- Armijo, R., Meyer, B., Navarro, S., King, G., Barka, A.: Asymmetric slip partitioning in the Sea of Marmara pull-apart; a clue to propagation processes of the North Anatolian Fault?, *Terra Nova*, 14, 80-86, 2002.

- Arpat, E., Şaroğlu, F.: Türkiye'deki bazı önemli genç tektonik olaylar [Some recent tectonic events in Turkey], Türkiye Jeoloji Kurumu Bülteni, 18, 91–101, 1975.
- Ateş, A., Kearey, P., and Tufan, S.: New gravity and magnetic anomaly maps of Turkey, *Geophys. J. Int.*, 136, 499–502, 1999.
- Baykal, F.: Sivas sheet of the Geological Map of Turkey, 1:500,000 scale, General Directorate of Mineral Research and Exploration, Ankara, 1961.
- Chaimov, T. A., Barazangi, M., al-Saad, D., Sawaf, T., and Gebran, A.: Mesozoic and Cenozoic deformation inferred from seismic stratigraphy in the southwestern intracontinental Palmyride fold-thrust belt, Syria, *Geol. Soc. Am. Bull.*, 104, 704–715, 1992.
- Demir, T., Westaway, R., Bridgland, D., Pringle, M., Yurtmen, S., Beck, A., and Rowbotham, G.: Ar-Ar dating of Late Cenozoic basaltic volcanism in northern Syria: implications for the history of incision by the River Euphrates and uplift of the northern Arabian Platform, *Tectonics*, 26, TC3012, doi:10.1029/2006TC001959, 2007.
- Kaymakçı, N., İnceöz, M., and Ertepinar, P.: 3D architecture and Neogene evolution of the Malatya Basin: inferences for the kinematics of the Malatya and the Ovacık fault zones, *Turk. J. Earth Sci.*, 15, 123–154, 2006.
- Le Pichon, X., Şengor, A. M. C., Demirbağ, E., Rangin, C., İmren, C., Armijo, R., Görür, N., Çağatay, N., Mercier de Lepinay, B., Meyer, B., Saatçılar, R., and Tok, B.: The active main Marmara Fault, *Earth Planet. Sci. Lett.*, 192, 595–616, 2001.
- Litak, R. K., Barazangi, M., Beauchamp, W., Seber, D., Brew, G., Sawaf, T., and Al-Youssef, W.: Mesozoic-Cenozoic evolution of the intraplate Euphrates fault system, Syria; implications for regional tectonics, *J. Geol. Soc. London*, 154, 653–666, 1997.
- McBride, J. H., Barazangi, M., Best, J., al-Saad, D., Sawaf, T., al-Otri, M., and Gebran, A.: Seismic reflection structure of intracratonic Palmyride fold-thrust belt and surrounding Arabian Platform, Syria, 74, 238–259, 1990.
- Önal, M.: Miocene stratigraphy and lignite potential of the northern part of the Malatya graben basin, East Anatolia-Turkey, in: *Proceedings of the International Earth Sciences Colloquium on the Aegean region (IESCA-1995)*, İzmir, 607–621, 1995.
- Önal, M.: Malatya Graben havzası güney bölümünün stratigrafisi ve depolanma ortamları: Cumhuriyet Üniversitesi Mühendisliği Fakültesi Dergisi, Series A, 14(1), 1–12, Sivas, 1997.
- Özgül, N.: Torosların bazı temel jeolojik özellikleri, Türkiye Jeoloji Kurumu Bülteni, 19, 65–78, 1976.
- Perinçek, D. and Kozlu, H.: Stratigraphy and structural units of the Afşin – Elbistan – Doğanşehir region (Eastern Taurus), in: *Geology of the Taurus Belt*, edited by: Tekeli, O., Göncüoğlu, M. C., *Proceedings of the 1983 Ankara Symposium*, General Directorate of Mineral Research and Exploration, Ankara, 181–198, 1984.
- Robertson, A. H. F., Unlügenç, U. C., İnan, N., and Taşlı, K.: The Misis-Andırın Complex: a Mid-Tertiary melange related to late-stage subduction of the Southern Neotethys in S Turkey, *J. Asian Earth Sci.*, 22, 413–453, 2004.
- Seyrek, A., Demir, T., Pringle, M., Yurtmen, S., Westaway, R., Beck, A., Rowbotham, G.: Kinematics of the Amanos Fault, southern Turkey, from Ar-Ar dating of offset Pleistocene basalt flows: transpression between the African and Arabian plates, in: *Tectonics of Strike-slip Restraining and Releasing Bends*, edited by: Cunningham, D. and Mann, P., Geological Society, London, Special Publication, 290, 255–284, 2007.
- Seyrek, A., Demir, T., Pringle, M., Yurtmen, S., Westaway, R., Bridgland, D., Beck, A., and Rowbotham, G.: Late Cenozoic uplift of the Amanos Mountains and incision of the Middle Ceyhan river gorge, southern Turkey; Ar-Ar dating of the Düziçi basalt, *Geomorphology*, 97, 321–355, 2008.
- Tezcan, A. K.: Geothermal explorations and heat flow in Turkey, in: *Terrestrial Heat Flow and Geothermal Energy in Asia*, edited by: Gupta, M. L. and Yamano, M., Science Publishers, Lebanon, New Hampshire, 23–42, 1995.
- Tolun, N.: Hatay sheet of the Geological Map of Turkey, 1:500,000 scale, General Directorate of Mineral Research and Exploration, Ankara, 1962.
- Tüysüz, O., Barka, A., and Yiğitbaş, E.: Geology of the Saros graben and its implications for the evolution of the North Anatolian fault in the Ganos-Saros region, northwestern Turkey, *Tectonophysics*, 293, 105–126, 1998.
- Ünay, E. and de Bruijn, H.: Plio-Pleistocene rodents and lagomorphs from Anatolia, in: *The Dawn of the Quaternary, Proceedings of the 1996 SEQS-EuroMam Symposium*, Mededelingen Nederlands Instituut voor Toegepaste Geowetenschappen TNO 60, 431–465, 1998.
- Westaway, R.: Kinematics of the Middle East and Eastern Mediterranean updated, *Turk. J. Earth Sci.*, 12, 5–46, 2003.
- Westaway, R.: Kinematic consistency between the Dead Sea Fault Zone and the Neogene and Quaternary left-lateral faulting in SE Turkey, *Tectonophysics*, 391, 203–237, 2004.
- Westaway, R.: Late Cenozoic extension in southwest Bulgaria: a synthesis, in: *Tectonic Development of the Eastern Mediterranean Region*, edited by: Robertson, A. H. F. and Mountrakis, D., *Geol. Soc., London, Special Publication* 260, 557–590, 2006.
- Westaway, R. and Arger, J.: The Gölbaşı basin, southeastern Turkey: A complex discontinuity in a major strike-slip fault zone, *J. Geol. Soc. London*, 153, 729–743, 1996.
- Westaway, R. and Arger, J.: Kinematics of the Malatya-Ovacık Fault Zone, *Geodinamica Acta*, 14, 103–131, 2001.
- Westaway, R., Demir, T., Seyrek, A., and Beck, A.: Kinematics of active left-lateral faulting in southeast Turkey from offset Pleistocene river gorges: improved constraint on the rate and history of relative motion between the Turkish and Arabian plates, *J. Geol. Soc. London*, 163, 149–164, 2006.
- Westaway, R., Guillou, H., Yurtmen, S., Demir, T., Scaillet, S., and Rowbotham, G.: Constraints on the timing and regional conditions at the start of the present phase of crustal extension in western Turkey from observations in and around the Denizli region, *Geodinamica Acta*, 18, 209–238, 2005.
- Yaltırak, C., Sakıncı, M., and Oktay, F. Y.: Comment on “Westward propagation of the North Anatolian fault into the northern Aegean: Timing and kinematics” by Armijo, R., Meyer, B., Hubert, A., Barka, A., *Geology*, 28, 187–188, 2000.
- Zor, E., Sandvol, E., Gürbüz, C., Türkelli, N., Seber, D., and Barazangi, M.: The crustal structure of the east Anatolian Plateau (Turkey) from receiver functions, *Geophys. Res. Lett.*, 30(24), 8044, doi:10.1029/2003GL018192, 2003.